# *In vitro* and *in vivo* irinotecan-induced changes in expression profiles of cell cycle and apoptosis-associated genes in acute myeloid leukemia cells

**Hans Minderman,[1] Jeffrey M. Conroy,[2] Kieran L. O'Loughlin,[1] Devin McQuaid,[2] Paul Quinn,[2] Song Li,[1] Lakshmi Pendyala,[1] Norma J. Nowak,[2] and Maria R. Baer[1]**

**Departments of [1]Medicine and [2]Cancer Genetics, Roswell Park Cancer Institute, Buffalo, New York**

## Abstract

**Objective: To study irinotecan (CPT-11)–induced changes in expression profiles of genes associated with cell cycle control and apoptosis in myeloid leukemia cells *in vitro* and *in vivo*. Methods: HL60 cells were exposed to clinically achievable concentrations of 7-ethyl-10-hydroxy-camptothecin (SN-38), the active metabolite of CPT-11, and blood sampled from patients with acute myeloid leukemia and chronic myeloid leukemia in myeloid blast transformation treated with CPT-11. Gene expression changes were studied by cDNA microarray and correlated with biological responses by studying DNA distributions by flow cytometry. Results: cDNA microarray analysis showed down-regulation and up-regulation of specific cell cycle–associated genes, consistent with loss of S-phase cells and temporary delay of $G_1$-S-phase transition seen by flow cytometry. Flow cytometry showed that cells in S phase during SN-38 exposure underwent apoptosis, whereas cells in $G_2$-M and $G_1$ were delayed in $G_1$ and entered S phase only 6 to 8 hours after drug removal, consistent with the observed changes in gene expression. Proapoptotic changes in gene transcription included down-regulation of antiapoptotic genes and up-regulation of proapoptotic genes. Many gene expression changes observed following *in vitro* SN-38 exposure were also seen following *in vivo* administration of 10 or 15 mg/m$^2$ CPT-11; notably, proapoptotic changes included reduced transcription of survivin pathway-associated genes and increased transcription of death receptor 5. Conclusion: CPT-11-induced changes in gene expression profiles *in vitro* and *in vivo* are consistent with temporary delay in $G_1$-S transition and enhanced responsiveness to apoptosis, both of which may contribute to the synergistic interactions of this drug with antimetabolites. [Mol Cancer Ther 2005;4(6):885–900]**

## Introduction

Irinotecan (CPT-11) is metabolized by carboxylesterases to its active metabolite 7-ethyl-10-hydroxycamptothecin (SN-38). SN-38 acts as a classic topoisomerase I inhibitor: it stabilizes the topoisomerase I/DNA cleavable complex, which blocks DNA replication and causes DNA strand breaks. Although CPT-11 has activity as a single agent in diverse malignancies (1–7), its major role seems to be in combination with other chemotherapy drugs.

The optimal sequence of administration of CPT-11 with other chemotherapy drugs has not been clearly established because mechanisms of synergy are incompletely understood. These mechanisms may be drug specific. For example, synergy of CPT-11 with thymidylate synthetase inhibitors, such as 5-fluorouracil, may be explained by prolonged inhibition of thymidylate synthetase and increased incorporation of 5-fluorouracil metabolites into DNA (8, 9). On the other hand, synergistic effects of CPT-11 may be associated with a more general cellular response. In this regard, CPT-11 has been reported to alter cell cycle kinetics (10) and also to augment the apoptotic response (11–17), for example, increasing apoptosis induced by tumor necrosis factor (TNF)–related apoptosis-inducing ligand/Apo2L by up-regulating death receptor 5 [TNF receptor superfamily 10B (TNFRSF10B); refs. 11, 13]. Preclinical data favor administration of CPT-11 prior to antimetabolites (14), which is a schedule consistent with both of these mechanisms of synergy.

Established determinants of response to CPT-11 include topoisomerase I expression levels, mutations of the *topoisomerase I* gene, and carboxylesterase activity. It has been suggested that differential drug sensitivity may also reflect molecular responses to DNA damage (18, 19), including cell cycle perturbations, apoptotic response, and DNA repair. Thus, evaluation of kinetic changes in molecular responses to CPT-11 or SN-38 may provide a rationale for optimizing scheduling of CPT-11 combination chemotherapy. The current study explores changes in gene transcription in HL60 cells exposed to SN-38 studied by cDNA microarray analysis using a customized gene array comprising 3,011 cancer-related genes. Kinetic changes in

Received 2/20/04; revised 4/6/05; accepted 4/13/05.

**Grant support:** National Cancer Institute grant R21 CA89938, Roswell Park Alliance Foundation grant, Roswell Park Cancer Center support grant P30 CA16056, Leonard S. LoVullo Memorial Fund for Leukemia Research, and Dennis J. Szefel, Jr., Endowed Fund for Leukemia Research at Roswell Park Cancer Institute.

The costs of publication of this article were defrayed in part by the payment of page charges. This article must therefore be hereby marked advertisement in accordance with 18 U.S.C. Section 1734 solely to indicate this fact.

**Requests for reprints:** Hans Minderman, Department of Medicine, Roswell Park Cancer Institute, Science Building 616, Elm and Carlton Streets, Buffalo, NY 14263. E-mail: hans.minderman@roswellpark.org

gene expression in blasts from patients with acute myeloid leukemia (AML) and chronic myeloid leukemia (CML) in myeloid blast transformation following *in vivo* therapy with a single dose of CPT-11 were then compared with the changes observed in HL60 cells following short-term *in vitro* SN-38 exposure.

## Materials and Methods

### Cell Line and Drug Exposure

HL60 cells were maintained in exponential growth in RPMI 1640 (Life Technologies, Grand Island, NY) supplemented with 10% heat-inactivated fetal bovine serum, 2 mmol/L L-glutamine, 20 units/mL penicillin, and 20 μg/mL streptomycin (Life Technologies) buffered in 5% $CO_2$ in air. The *in vitro* studies were done on asynchronously growing HL60 cells to ensure that changes in gene transcription could be attributed to exposure to SN-38 rather than to prior cell synchronization. A stock solution of 5 mmol/L SN-38 (Pharmacia Co., Kalamazoo, MI) was prepared in 100% DMSO and stored in aliquots at −20°C. SN-38 from the frozen stock was added to cells cultured at $1 \times 10^6$/mL to achieve the desired final concentrations. Two separate series of drug exposures were done. In the first series of experiments, HL60 cells were exposed to 0, 0.1, and 0.3 μmol/L SN-38 for 2 hours. In the second series of experiments, cells were exposed to 0, 0.1, 0.3, and 1.0 μmol/L SN-38 for 2 hours to establish reproducibility of results and to extend the drug concentration range. Cells were incubated with drug at 37°C for 2 hours, washed twice with PBS, resuspended in supplemented RPMI 1640 at $0.25 \times 10^6$ cells/mL, and incubated at 37°C in a fully humidified atmosphere of 5% $CO_2$ in air.

Cell aliquots required for each assay were removed from the cultures at the time intervals indicated in Results. For cDNA microarray analysis, $1 \times 10^7$ cells per sample point were cryopreserved at −80°C in 20% DMSO in supplemented RPMI 1640 using controlled cooling (Nalgene Cryo 1°C freezing container, Nalge Nunc International, Naperville, IL). For flow cytometric DNA distribution analyses, $1 \times 10^6$ cells per sample point were fixed in 70% ice-cold ethanol.

### Patient Samples

A patient with refractory AML (WBC count $24 \times 10^9$ cells/L, with 88% blasts) and a patient with refractory CML in myeloid blast transformation (WBC count $42 \times 10^9$ cells/L, with 89% blasts) received 10 and 15 mg/m$^2$ CPT-11, respectively, over 90 minutes daily for 5 days, with 1 g/m$^2$ cytarabine (Ara-C) 12 hours after each CPT-11 dose, on a Roswell Park Cancer Institute phase I protocol (RPC 9901). Peripheral blood was sampled following the first CPT-11 dose at the times detailed in Results. Samples were enriched for nucleated cells by ammonium chloride lysis and then cryopreserved in 20% DMSO. The study was approved by the Roswell Park Cancer Institute Scientific Review Committee and Institutional Review Board.

### Experimental Design for Microarray Analysis

HL60 cells were cultured without drug (control) and with SN-38 at 0.1, 0.3, and 1.0 μmol/L for 2 hours. The microarray analysis compared gene transcription profiles of drug-treated cells to those of control cells sampled at the same time points. Time points of blood samples obtained from the two patients after the start of the CPT-11 infusion were the same as the HL60 sampling time points. For the patient samples, the microarray analysis compared gene transcription profiles of cells sampled following drug exposure to that of a sample taken immediately before the start of the infusion.

### RNA Preparation

Total RNA was extracted using RNeasy Midi kits (Qiagen, Inc., Valencia, CA) according to manufacturer's instructions. After elution, RNA samples were concentrated by ethanol precipitation at −20°C overnight and resuspended in nuclease-free water. Before labeling, RNA was measured with a Genequant spectrophotometer (Amersham Biosciences, Piscataway, NJ) and evaluated for degradation with a 2100 Bioanalyzer (Agilent, Palo Alto, CA). Only samples with $A_{260/280\ nm}$ ratios of 1.9–2.0 and 28S:18S ribosomal band ratios of >1.5 were analyzed.

### Production of cDNA Microarrays

The cancer-specific arrays used in this study were produced in the Roswell Park Cancer Institute Microarray and Genomics Core Facility. cDNA clones ($n$ = 3,011; Research Genetics, Huntsville, AL) were selected based on their association with oncogenesis. Each clone was amplified from 100 ng bacterial DNA by PCR amplification of the insert using M13 universal primers for the plasmids represented in the clone set (5′-TGAGCGGATAACAATTTCACACAG-3′ and 5′-GTTTTCCCAGTCACGACGTTG-3′). Each PCR product (75 μL) was purified by ethanol precipitation, resuspended in 25% DMSO, and adjusted to 200 ng/μL. Printing solutions were spotted in triplicate on type A glass slides (Schott Nexterion, Duryea, PA) using a MicroGrid II TAS arrayer and MicroSpot 2500 split pins (Genomic Solutions, Inc., Ann Arbor, MI).

### Preparation and Hybridization of Fluorescent-Labeled cDNA

cDNAs were synthesized and indirectly labeled using the Atlas Powerscript Fluorescent Labeling kit (BD Biosciences Palo Alto, CA). Total RNA from drug-exposed cells and untreated (no drug) reference cells was labeled with Cy5 and Cy3, respectively. For each reverse transcription reaction, total RNA (2.5 μg) was mixed with 2 μL random primers (Invitrogen, Carlsbad, CA) in a total volume of 10 μL, heated to 70°C for 5 minutes, and cooled to 42°C. To this sample was added an equal volume of reaction mix (4 μL of 5× First-Strand buffer, 2 μL of 10× deoxynucleotide triphosphate mix, 2 μL DTT, 1 μL deionized $H_2O$, and 1 μL Powerscript Reverse Transcriptase) per manufacturer's instructions. After 1-hour incubation at 42°C, the RNA was degraded by 70°C incubation for 5 minutes. The mixture was cooled to 37°C and incubated for 15 minutes

with 0.2 μL RNase H (10 units/μL). The resultant amino-modified cDNA was purified, precipitated, and fluoresceinated as described by the manufacturer. Uncoupled dye was removed from the labeled probe by washing thrice using a Qiaquick PCR Purification kit (Qiagen). The probe was then eluted in 60 μL elution buffer and dried down to completion in a SpeedVac.

Because of low RNA yields, the RNA extracted from the AML patient samples was amplified and labeled using the Atlas SMART Fluorescent Probe Amplification kit (Becton Dickinson, Franklin Lakes, NJ; refs. 20, 21) according to the manufacturer's instructions. This amplification was shown not to alter the relative gene expressions by comparing the expression profiles of amplified and unamplified genes in HL60 cells over the entire time course following exposure to 0.3 μmol/L SN-38 (data not shown). Amplified cDNA (2 μg) was then amino-modified and purified before coupling to Cy3- or Cy5-reactive dye (Amersham Biosciences) with the reagents supplied in the Atlas kit. The labeled probe was purified, eluted, and dried as described previously for the unamplified samples.

Before hybridization, the two separate probes were resuspended in 10 μL deionized $H_2O$, combined, and mixed with 2 μL human Cot-1 (20 μg/μL, Invitrogen) and 2 μL poly(A) (20 μg/μL, Sigma, St. Louis, MO). The probe mixture was denatured at 95°C for 5 minutes, placed on ice for 1 minute, and prepared for hybridization with addition of 110 μL preheated (65°C) SlideHyb # 3 buffer (Ambion, Inc., Austin, TX). After a 5-minute incubation at 65°C, the probe solution was placed on the array in an assembled GeneTAC hybridization station module (Genomic Solutions). The slides were incubated at 55°C for 16 to 18 hours with occasional pulsation of the hybridization solution. After hybridization, the slides were washed in the automated GeneTAC station with reducing concentrations of SSC and SDS. The final wash was 30 seconds in 0.1× SSC followed by a 5-second 100% ethanol dip. The slides were spun dry and scanned immediately on an Affymetrix 428 laser scanner to generate two 10 μmol/L images, one for Cy3 and one for Cy5. Two hybridizations were done for each RNA sample, switching the dyes in the second hybridization to account for possible dye bias.

### Image Analysis

The hybridized slides were scanned using an Affymetrix 428 scanner to generate high-resolution (10 μm) images for both Cy3 and Cy5 channels. Image analysis was done on the raw image files using ImaGene (version 4.1, BioDiscovery, Inc., El Segundo, CA). Each cDNA spot was defined by a circular region. The size of the region was programmatically adjusted to match the size of the spot. Local background for a spot was determined by ignoring a 2- to 3-pixel buffer region around the spot and then measuring signal intensity in a 2- to 3-pixel area outside the buffer region. Raw signal intensity values for each spot and its background region were segmented using a proprietary optimized segmentation algorithm, which excludes pixels that are not representative of the majority of pixels in that region. The background-corrected signal for each cDNA spot is the mean signal (of all the pixels in the region) minus the mean local background. The output of the image analysis is two tab-delimited files, one for each channel, containing all of the raw fluorescence data.

### Data Analysis

The output of the image analysis was processed by a Perl program developed at Roswell Park Cancer Institute. Spots that were not significantly above background or had a poor coefficient of variance were excluded. For each spot, the ratio of the background-subtracted mean signals of the two channels was calculated. The ratios were then normalized on the log scale across the entire slide. For each slide, the expression ratios were defined as the $\log_2$ mean of all replicate spots. The results from the two slides that make up the dye swap were then averaged on the log scale and became the final expression ratio of that clone. Hierarchical clustering analysis was done with Stanford's Genecluster software version 2.12. The genes were filtered to only include those that appeared in at least 50% of the time points and had at least a 2-fold differential expression (up or down) at at least one time point. The raw and processed electronic files associated with all of the data presented are available.[3] Detailed evaluation of gene expression time kinetics included all genes for which the $\log_2$ of the expression ratio of drug-treated to control cells was >0.9 (1.87-fold increase) or less than −0.9 (1.87-fold decrease) at at least one time point (arbitrary thresholds). Expression ratios were plotted against sampling time using Sigma Plot version 8.0 software (Jandell, San Rafael, CA).

### Validation Using Real-time Quantitative Reverse Transcription-PCR

The mRNA levels of survivin and TNF (ligand) superfamily member 9 (TNFSF9) in HL60 cells following exposure to 0, 0.1, 0.3, and 1.0 μmol/L SN-38 were validated using real-time quantitative reverse transcription-PCR (Taqman assay) with a Perkin-Elmer (Boston, MA) ABI PRISM Sequence Detection System. The mRNA level of each gene is expressed relative to that of the endogenous standard (β-actin) measured concurrently from the same RNA extracts and cDNA preparations. cDNA for these experiments was synthesized using SuperScript II reverse transcriptase. The comparative $C_T$ method of quantitation was used as described previously (22). The results are presented as mRNA expression values relative to that of β-actin. The primers and probes for survivin, TNFSF9 and β-actin were purchased from Applied Biosystems, Inc. (Foster City, CA) as ready-to-use kits.

### DNA Distribution Analysis

Aliquots of $1 \times 10^6$ cells were harvested at the indicated time intervals, fixed in ice-cold 70% (v/v) ethanol/distilled water, and stored at −20°C. Cell pellets were rehydrated by washing twice in PBS and then resuspended for 30 minutes in 1 mL propidium iodide staining buffer [0.05 mg/mL propidium iodide (Molecular Probes, Eugene, OR), 0.1% sodium citrate, 0.02 mg/mL RNase A, 0.37% NP40 (pH 7)]

[3] http://microarrays.roswellpark.org/supplemental/Minderman

on ice. Cell pellets were washed twice with PBS and then analyzed on a FACScan flow cytometer to assess DNA content. DNA distribution histograms from the flow cytometry data were produced with the WinList software program (Verity Software House, Topsham, ME).

### Bromodeoxyuridine Labeling

A separate set of experiments was set up to study cells that were in S phase during drug exposure. Cells were labeled with bromodeoxyuridine (BrdUrd; 10 μmol/L, 20 minutes; Roche, Mannheim, Germany), washed with PBS, and then exposed to SN-38 for 2 hours. Following the 2-hour exposure to SN-38, cells were washed twice and cell aliquots ($1 \times 10^6$) were harvested at the indicated time intervals, fixed in ice-cold 70% (v/v) ethanol/distilled water, and stored at −20°C. BrdUrd labeling was visualized with a fluorescein-labeled anti-BrdUrd monoclonal antibody (Roche Diagnostics Corporation/Roche Applied Science, Indianapolis, IN) according to the manufacturer's instructions. Bivariate analysis of BrdUrd/propidium iodide staining was done as described previously (23).

## Results

### Reproducibility of cDNA Microarray Analysis

The technical reproducibility of the cDNA microarray analysis was first assessed by a dye-swap study in which the Cy3 and Cy5 labels were interchanged in two preparations of the same sample to show lack of dye bias. Dye swaps in three independently prepared samples of HL60 cells in logarithmic phase yielded $r^2$ correlation coefficients of 0.92, 0.89, and 0.95, indicating excellent correlation.

Biological reproducibility was assessed by comparing three independently prepared samples of HL60 cells in logarithmic growth. The gene transcription profile of each preparation was compared with that of the other two; the three possible hybridization combinations yielded $r^2$ correlation coefficients of 0.92, 0.96, and 0.94, indicating excellent correlation.

### Hierarchical Clustering Analysis of Gene Transcription Profiles in HL60 Cells Exposed to SN-38

Hierarchical clustering, applying an arbitrary filter to only include those genes that appeared in at least 50% of the time points and had at least a 2-fold differential expression (up or down) at at least one time point, identified groups of genes with similar kinetic patterns of gene expression in drug-treated cells (Fig. 1). However, the function of the genes comprising each group was heterogeneous (data not shown), indicating that hierarchical clustering of gene expression ratios may not be the optimal approach to identifying biologically relevant associations.

### Kinetic Analysis of Transcription of Genes Associated with Cell Cycle Control and Apoptosis

In addition to the hierarchical clustering analysis, which groups genes according to similarities in kinetic changes in gene expression, the data were also analyzed by grouping genes according to biological function. Diverse gene transcription profiles, including both increases and decreases in expression, were observed within biological function groups. In addition, among genes with a single type of response (increase or decrease), different time kinetics were observed.

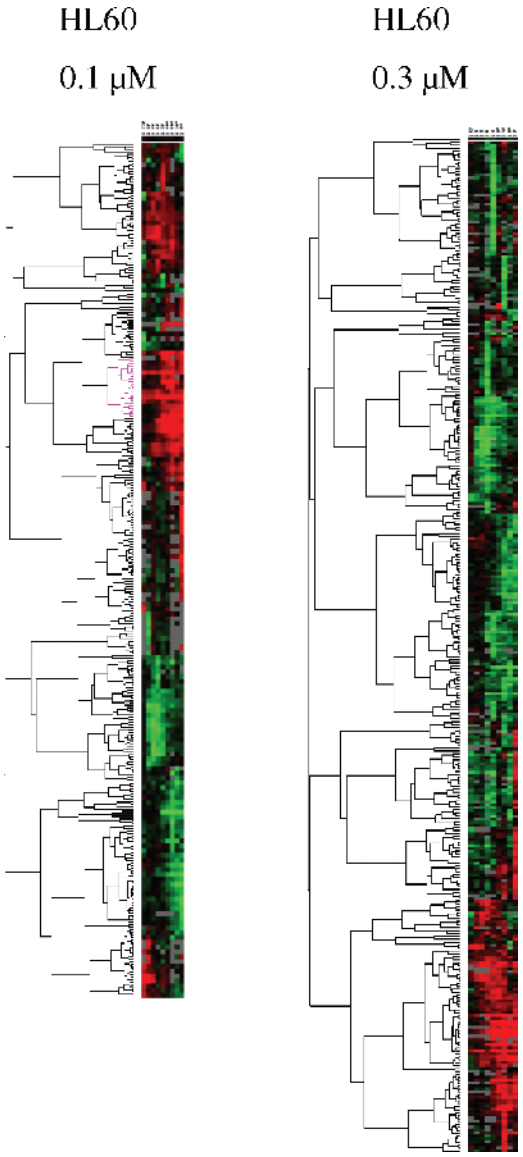


**Figure 1.** Hierarchical clustering analysis of gene expression kinetics in HL60 cells following 2-h exposure to 0.1 and 0.3 μmol/L SN-38. Each *line* represents an individual gene and consists of individual squares corresponding to the sampling time points, whose color represents the ratio of expression in drug-treated compared with control cells studied at the same time point. Genes for which the $\log_2$ of this ratio exceeded 1 (at least 2-fold increase) or was less than −1 (at least 2-fold decrease). Relative overexpression and underexpression compared with control are shown in *red* and *green*, respectively.

Notable changes in transcription of cell cycle–associated genes (arbitrary threshold >1.87-fold increase or decrease compared with control) included down-regulation of *cyclin A2*, *cell division cycle (CDC) 2*, *CDC7-like 1*, *cyclin F*, *CDC27*, *centromere protein E*, and *kinesin-like 5*, with recovery

to control values 12 hours following drug exposure (Fig. 2). *v-abl Abelson murine leukemia viral oncogene homologue 1* and *cyclin-dependent kinase (CDK) 4* were also down-regulated, but for a shorter period. *BTG family member 2* was up-regulated for at least 12 hours after drug removal. In contrast, *B-cell chronic lymphocytic leukemia (CLL)/lymphoma (BCL) 6* and *CDK inhibitor 2A (p16)* were also up-regulated but quickly returned to control levels.

With the same arbitrary threshold of >1.87-fold increase or decrease compared with control, the apoptosis-associated genes *BCL10*, *BCL2/adenovirus E1B 19-kDa interacting protein 3*, *TNFSF9*, and *caspase-6 apoptosis-related cysteine protease* were all rapidly up-regulated (within 2 hours of drug removal) and returned to control levels within 8 to 12 hours after drug removal (Fig. 3). *TNFRSF10B (death receptor 5)* and *BCL2-related protein A1* were also up-regulated, but transcription peaked 4 to 6 hours after drug removal. Three different patterns of down-regulation of genes associated with apoptosis were also observed. *BCL2* and *TNF receptor–associated factor (TRAF) family member–associated nuclear factor-κB activator* were down-regulated immediately after drug removal and gradually recovered to control levels over the sampling period. *Baculoviral IAP repeat–containing 5 [BIRC5 (survivin)]* transcription decreased gradually, nadired 8 hours after drug removal, and then recovered over the next 6 hours. *BCL2-like 2* was quickly down-regulated but returned to control levels within 2 hours.

### Dose-Dependent Effects on Gene Transcription

More genes were affected by incubation with 0.3 μmol/L compared with 0.1 μmol/L SN-38. Using the arbitrary threshold of a 1.87-fold difference in transcription, 488 genes were affected by incubation with 0.3 μmol/L SN-38 compared with 368 with 0.1 μmol/L SN-38, but the number of genes affected was not greater with 1 μmol/L SN-38 (453 genes). Using the same arbitrary threshold of a 1.87-fold difference in transcription, 65 genes were affected by exposure to SN-38 at all three concentrations: 28 were up-regulated (Table 1) and 37 were down-regulated (Table 2). There were no appreciable differences in the extent or duration of transcriptional changes of these genes at the different drug concentrations used (data not shown).

### Gene Transcription following *In vivo* Exposure to 10 and 15 mg/m$^2$ CPT-11

To determine whether the gene transcription changes induced by SN-38 *in vitro* were also induced *in vivo*,

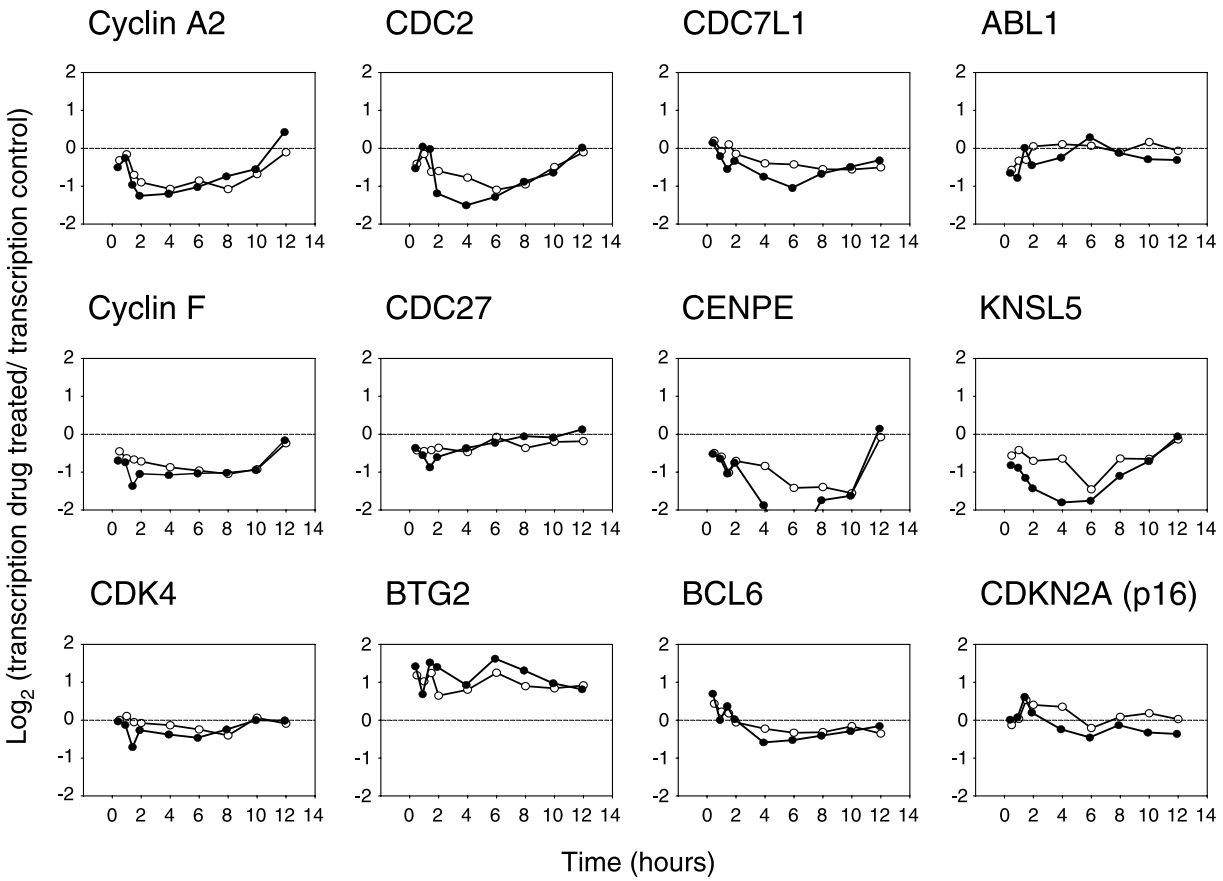


**Figure 2.** Time kinetic analysis of transcription of genes associated with cell cycle control. $Log_2$ of the ratios of expression levels of cells treated with 0.1 μmol/L (○) and 0.3 μmol/L (●) SN-38 compared with control cells.

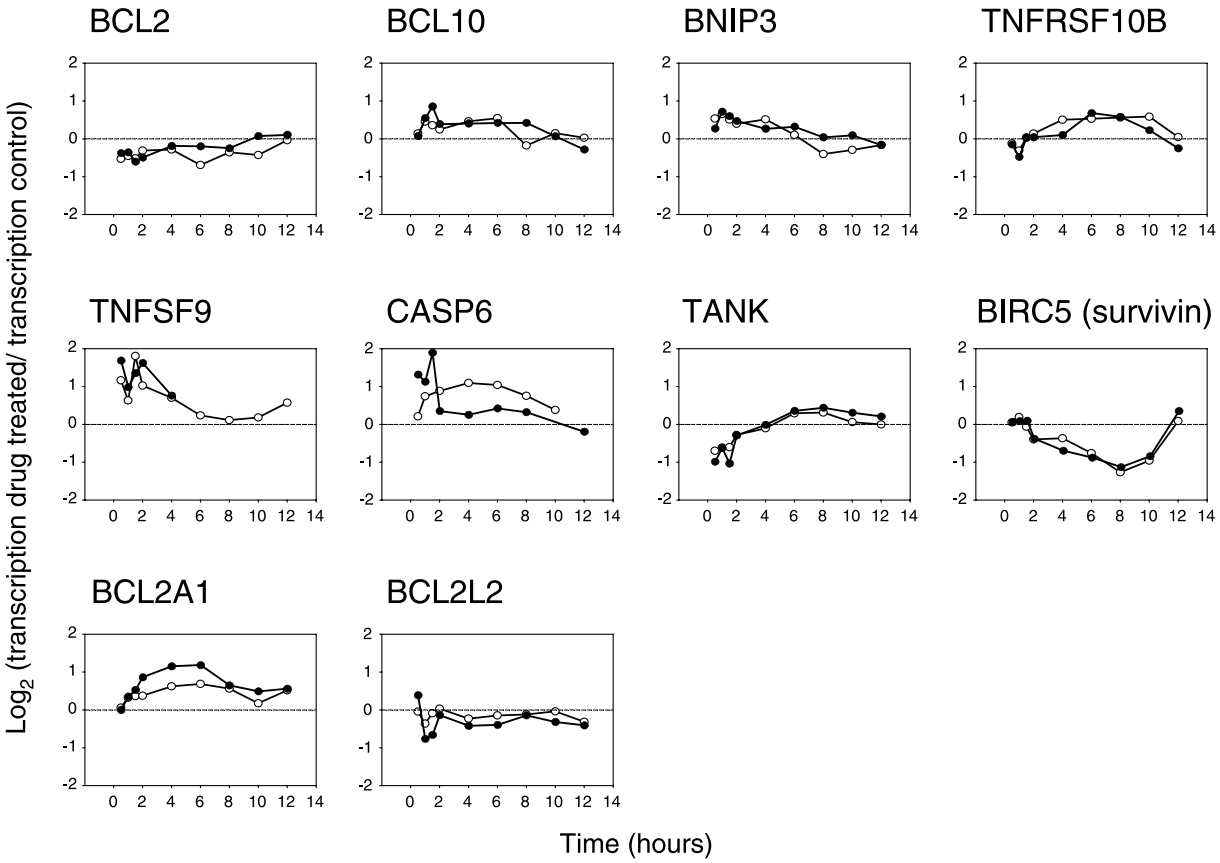


**Figure 3.** Time kinetic analysis of transcription of genes associated with apoptosis. $Log_2$ of the ratios of expression levels of cells treated with 0.1 μmol/L (○) and 0.3 μmol/L (●) SN-38 compared with control cells.

gene transcription was studied in peripheral blasts from two leukemia patients treated with CPT-11. Using the same arbitrary threshold as used for the HL60 data (1.87-fold difference in transcription), 58 genes were found to be up-regulated (Table 3) and 64 genes were down-regulated (Table 4) in cells of the CML patient treated with 15 mg/m$^2$ dose, whereas in the AML patient treated with the 10 mg/m$^2$ dose ~1,230 genes were up-regulated and 777 genes were down-regulated (not filtered for overlapping clones identifying the same gene). It is unclear why the number of affected genes in the AML patient were much higher than those observed in the HL60 cells *in vitro* and the CML patient *in vivo*. Although preliminary data have shown that the RNA amplification method used for this patient's samples did not affect relative gene expression levels in HL60 cells, a contribution of the amplification to these results cannot be ruled out definitively.

Kinetic gene expression data were compared among seven data sets: two data sets each for HL60 cells exposed to 0.1 and 0.3 μmol/L SN-38, one data set for HL60 cells exposed to 1.0 μmol/L SN-38, one data set for the AML patient treated with 10 mg/m$^2$ CPT-11, and one data set for the CML patient treated with 15 mg/m$^2$ CPT-11. These data sets were correlated with regard to the extent of treatment-induced changes using Microsoft Access software. Table 5 (up-regulation) and Table 6 (down-regulation) show the results of queries for similarities in changes in gene expression, applying a range of threshold values. When the arbitrary threshold of >1.87-fold difference was applied (as used for the analysis of the HL60 data), only eight genes were similarly affected in all seven data sets. The number of genes similarly affected increased rapidly with decreasing threshold values.

Notably, one of the genes that were down-regulated both *in vitro* and *in vivo* was *survivin*, which is one of only four recognized transcriptomes (genes selectively expressed in human tumors but undetectable or found at very low levels in normal tissue isolated from the same organ; ref. 22). We therefore analyzed the transcription of survivin pathway-associated genes following *in vitro* SN-38 (Fig. 4) and *in vivo* CPT-11 (Fig. 5) exposure and found that all were down-regulated both *in vitro* and *in vivo*. Some differences were observed between the two patients (Fig. 5), notably with regard to the degree of down-regulation of *serine/threonine kinase 12* transcription and the duration of down-regulation of the other genes. The observed differences may reflect interpatient

**Table 1. Genes up-regulated at least 1.87-fold during at least one time point following exposure to 0.1, 0.3, and 1.0 μmol/L SN-38**

| No. | Clone ID | Gene |
|---|---|---|
| 1 | H21042 | *Activating transcription factor 3* |
| 2 | T63779 | *Basic transcription element binding protein 1* |
| 3 | AA279755 | *CD69 antigen (p60, early T-cell activation antigen)* |
| 4 | AA759046 | *Dual-specificity phosphatase 2* |
| 5 | AA486533 | *Early growth response 1* |
| 6 | H72122 | *Ectodermal-neural cortex (with BTB-like domain)* |
| 7 | AI123732 | *EBV-induced gene 2 (lymphocyte-specific G protein–coupled receptor)* |
| 8 | T61948 | *FBJ murine osteosarcoma viral oncogene homologue B* |
| 9 | R42479 | *Human ETS2 oncogene* |
| 10 | AA150507 | *Interleukin-1β* |
| 11 | T99236 | *junB proto-oncogene* |
| 12 | T72581 | *Matrix metalloproteinase 9 (gelatinase B, 92-kDa gelatinase, 92-kDatype IV collagenase)* |
| 13 | AA458838 | *Phorbol 12-myristate 13-acetate-induced protein 1* |
| 14 | AA436163 | *Prostaglandin E synthase* |
| 15 | R02740 | *Putative chemokine receptor; GTP-binding protein* |
| 16 | AA017544 | *Regulator of G protein signaling 1* |
| 17 | AA486277 | *Retinoblastoma-binding protein 5* |
| 18 | AI375353 | *Serum/glucocorticoid–regulated kinase* |
| 19 | AA418813 | *Splicing factor, arginine/serine–rich 7 (35 kDa)* |
| 20 | AA398458 | *Sulfotransferase family, cytosolic, 1A, phenol-preferring member 3* |
| 21 | R71691 | *TRAF1* |
| 22 | AA490213 | *Transducer of ERBB2, 1* |
| 23 | AA879435 | *Transducer of ERBB2, 2* |
| 24 | AA954188 | *Tubulin-specific chaperone c* |
| 25 | AA778663 | *TNFSF9* |
| 26 | H96235 | *v-ets avian erythroblastosis virus E26 oncogene homologue 2* |
| 27 | AA485377 | *v-fos FBJ murine osteosarcoma viral oncogene homologue* |
| 28 | W96155 | *v-jun avian sarcoma virus 17 oncogene homologue* |

variability and/or different doses received (10 versus 15 mg/m$^2$). Nevertheless, the data in Figs. 4 and 5 show compelling similarities in the kinetic changes in transcription of genes in this specific biological pathway *in vitro* and *in vivo*.

### Validation Using Real-time Quantitative Reverse Transcription-PCR

mRNA expression of representative down-regulated (*survivin*) and up-regulated (*TNFSF9*) genes in HL60 cells as detected by microarray analysis was validated by quantitative reverse transcription-PCR. Expression levels were determined 6 hours following a 2-hour exposure to 0, 0.1, 0.3, or 1.0 μmol/L SN-38 and are presented as ratios to the endogenous β-actin control. The data in Table 7 confirm the SN-38-induced changes in expression levels as observed with the microarray studies. However, whereas no appreciable dose-dependent effects

**Table 2. Genes down-regulated at least 1.87-fold during at least one time point following exposure to 0.1, 0.3, and 1.0 μmol/L SN-38**

| No. | Clone ID | Gene |
|---|---|---|
| 1 | AA455997 | *Adenomatosis polyposis coli* |
| 2 | AA460685 | *BIRC5 (survivin)* |
| 3 | AA446462 | *Budding uninhibited by benzimidazoles 1 (yeast homologue)* |
| 4 | N50544 | *c-myc promoter-binding protein* |
| 5 | AA278384 | *CDC2, $G_1$-S and $G_2$-M* |
| 6 | AA489042 | *CDC2-like 5 (cholinesterase-related cell division controller)* |
| 7 | AA448659 | *CDC25B* |
| 8 | AA411850 | *Centromere protein E (312 kDa)* |
| 9 | AA701455 | *Centromere protein F (350/400 kDa, mitosin)* |
| 10 | H99736 | *Chromodomain helicase DNA-binding protein 1* |
| 11 | AA022480 | *Cyclic AMP–responsive element binding protein-binding protein (Rubinstein-Taybi syndrome)* |
| 12 | AA608568 | *Cyclin A2* |
| 13 | AA774665 | *Cyclin B2* |
| 14 | AA676797 | *Cyclin F* |
| 15 | AA284072 | *CDK inhibitor 3 (CDK2-associated dual-specificity phosphatase)* |
| 16 | AA676749 | *Dual-specificity tyrosine phosphorylation–regulated kinase 1A* |
| 17 | N94428 | *E1A binding protein p300* |
| 18 | N92519 | *E2F transcription factor 3* |
| 19 | AA983191 | *ets variant gene 6 (TEL oncogene)* |
| 20 | AA452933 | *H2A histone family member L* |
| 21 | R10285 | *Hyaluronan-mediated motility receptor (RHAMM)* |
| 22 | AA481076 | *MAD2 (mitotic arrest deficient, yeast, homologue)–like 1* |
| 23 | AA488610 | *Minichromosome maintenance deficient (Saccharomyces cerevisiae) 4* |
| 24 | AI268273 | *Mitogen-activated protein kinase kinase kinase 5* |
| 25 | AA280214 | *NCK adaptor protein 1* |
| 26 | AA664219 | *Nuclear receptor subfamily 3, group C, member 1* |
| 27 | AA453293 | *Phosphodiesterase 4B, cyclic AMP–specific [dunce (Drosophila) homologue phosphodiesterase E4]* |
| 28 | AA629262 | *Polo (Drosophila)–like kinase* |
| 29 | N39611 | *Replication factor C (activator 1) 3 (38 kDa)* |
| 30 | AA128328 | *Retinoblastoma-binding protein 1* |
| 31 | H84048 | *Retinoblastoma-like 1 (p107)* |
| 32 | AA425746 | *runt-related transcription factor 1 (aml1 oncogene)* |
| 33 | AA071486 | *Serine/threonine kinase 12* |
| 34 | R71691 | *TRAF1* |
| 35 | AA026682 | *Topoisomerase (DNA) IIα (170 kDa)* |
| 36 | AA430504 | *Ubiquitin carrier protein E2-C* |
| 37 | R25397 | *v-yes-1 Yamaguchi sarcoma viral oncogene homologue 1* |

**Table 3. Genes up-regulated at least 1.87-fold during at least one time point in a CML patient following *in vivo* treatment with 15 mg/m$^2$ CPT-11**

| No. | Clone ID | Gene |
|---|---|---|
| 1 | H21042 | *Activating transcription factor 3* |
| 2 | AA872001 | *Annexin A6* |
| 3 | AA281616 | *AT-binding transcription factor 1* |
| 4 | AA281583 | *BCL7A* |
| 5 | AA864861 | *BCL9* |
| 6 | AA778392 | *BENE protein* |
| 7 | AA779480 | *Bone morphogenetic protein 8 (osteogenic protein 2)* |
| 8 | AA983817 | *CD80 antigen (CD28 antigen ligand 1, B7-1 antigen)* |
| 9 | AA036881 | *Chemokine (C-C motif) receptor 1* |
| 10 | H99676 | *Collagen, type VI, α1* |
| 11 | AI086446\| AI939360 | *CDK5, regulatory subunit 2 (p39)* |
| 12 | AA406485 | *Cytochrome b5 outer mitochondrial membrane precursor* |
| 13 | AA448157 | *Cytochrome P450, subfamily I (dioxin inducible), polypeptide 1 (glaucoma 3, primary infantile)* |
| 14 | AA489234 | *Cytokine-inducible kinase* |
| 15 | AA410404 | *Damage-specific DNA-binding protein 2 (48 kDa)* |
| 16 | R00855 | *Dystrophia myotonica–containing WD repeat motif* |
| 17 | H49053 | *Expressed sequence tags, moderately similar to E3KARP (Homo sapiens)* |
| 18 | AA430675 | *Fanconi anemia, complementation group G* |
| 19 | W51760 | *Fibroblast growth factor 2 (basic)* |
| 20 | R62612 | *Fibronectin 1* |
| 21 | AA626797 | *G protein–coupled receptor 39* |
| 22 | AA664180 | *Glutathione peroxidase 3 (plasma)* |
| 23 | AA490613 | *H2A histone family member X* |
| 24 | H70473 | *Histidine-rich glycoprotein* |
| 25 | AA454079 | *H. sapiens mRNA; cDNA DKFZp761M02121 (from clone DKFZp761M02121); complete cds* |
| 26 | AA505045 | *Human L2-9 transcript of unrearranged immunoglobulin V(H)5 pseudogene* |
| 27 | AA455156 | *Hypothetical protein FLJ21019* |
| 28 | AA456321 | *Insulin-like growth factor 1 (somatomedin C)* |
| 29 | N64384 | *Integrin, αX (antigen CD11C (p150), αpolypeptide)* |
| 30 | AA282537 | *MADS box transcription enhancer factor 2, polypeptide B (myocyte enhancer factor 2B)* |
| 31 | AA227885 | *mal, T-cell differentiation protein* |
| 32 | R80235 | *Mouse double minute 2, human homologue of p53-binding protein* |
| 33 | AA709414 | *Nidogen (enactin)* |
| 34 | H72030 | *Nuclear domain 10 protein* |
| 35 | AA495962 | *Nuclear receptor coactivator 1* |
| 36 | AA909184 | *Oncostatin M receptor* |
| 37 | AA253430 | *Prefoldin 4* |
| 38 | AA450062 | *Prostate differentiation factor* |
| 39 | AI016085 | *Protein tyrosine phosphatase, nonreceptor type 22 (lymphoid)* |
| 40 | AA733105 | *Protein tyrosine phosphatase, receptor type, D* |
| 41 | R45941 | *Protein tyrosine phosphatase, receptor type, N* |
| 42 | AA478467 | *Protocadherin γsubfamily A, 1* |
| 43 | N51095 | *ras-related C3 botulinum toxin substrate 3 (rho family, small GTP-binding protein Rac3)* |
| 44 | N47967 | *Rho GTPase-activating protein 5* |
| 45 | AA004638 | *Ribosomal protein L4* |
| 46 | AA521346 | *Serine/threonine protein kinase* |
| 47 | AA460152 | *Serum-inducible kinase* |
| 48 | W44701 | *Solute carrier family 25 (mitochondrial carrier; adenine nucleotide translocator) member 6* |
| 49 | N71628 | *Spi-B transcription factor (Spi-1/PU.1 related)* |
| 50 | AA148737 | *Syndecan 4 (amphiglycan, ryudocan)* |
| 51 | AI057267 | *Thy-1 cell surface antigen* |
| 52 | AA916906 | *TNFRSF1A-associated via death domain* |
| 53 | N59881 | *Transferrin receptor (p90, CD71)* |
| 54 | AI347622 | *TNFSF7* |
| 55 | AA778663 | *TNFSF9* |
| 56 | AI253036\| AI793236 | *v-erb-a avian erythroblastic leukemia viral oncogene homologue-like 4* |
| 57 | W96155 | *v-jun avian sarcoma virus 17 oncogene homologue* |
| 58 | H59758 | *v-raf murine sarcoma 3611 viral oncogene homologue 1* |

*Continued*

in extent of the changes were observed with the microarray studies, the reverse transcription-PCR results did show a dose-dependent effect, indicating that the latter has a superior quantitative detection sensitivity.

### DNA Distributions and the Fate of S-Phase Cells in Asynchronous HL60 Cells following Exposure to SN-38

We sought to correlate the observed changes in gene expression with biological effects. To this end, analysis of DNA distribution was done, providing information on both cell cycle kinetics and apoptosis. The DNA distribution histograms of HL60 cells exposed to SN-38 for 2 hours are shown in Fig. 6. Although the DNA distribution of the untreated (control) cells did not change over time, a dose-dependent loss of cells with S-phase DNA content was seen following treatment, accompanied by a gain of cells with a sub-$G_1$ (apoptotic) DNA content. The loss of cells with S-phase DNA content resolved over time due to recruitment of cells from the $G_1$ phase.

BrdUrd labeling of S-phase cells before SN-38 exposure allowed determination of the fate of cells in S phase during SN-38 exposure. The bivariate plots of BrdUrd/propidium iodide labeling (Fig. 7) unequivocally show that, whereas the BrdUrd-labeled cells in the control cultures traverse the cell cycle, the BrdUrd-labeled cells following SN-38

**Table 4. Genes down-regulated at least 1.87-fold during at least one time point in a CML patient following *in vivo* treatment with 15 mg/m$^2$ CPT-11**

| No. | Clone ID | Gene |
|---|---|---|
| 1 | R21506 | *A kinase (PRKA) anchor protein 10* |
| 2 | AA461325 | *Adducin 3 (γ)* |
| 3 | N26688 | *Adenomatosis polyposis coli* |
| 4 | AA664101 | *Aldehyde dehydrogenase 1 family member A1* |
| 5 | AA460685 | *BIRC5 (survivin)* |
| 6 | AA446462 | *Budding uninhibited by benzimidazoles 1 (yeast homologue)* |
| 7 | AA480880 | *Butyrate response factor 2 (epidermal growth factor response factor 2)* |
| 8 | AA598974 | *CDC2, $G_1$-S and $G_2$-M* |
| 9 | AA411850 | *Centromere protein E(312 kDa)* |
| 10 | N57964 | *Chemokine (C-C motif) receptor 6* |
| 11 | H73968 | *Chromosome 20 open reading frame 1* |
| 12 | AA608568 | *Cyclin A2* |
| 13 | R46787 | *Cyclin B1* |
| 14 | AA774665 | *Cyclin B2* |
| 15 | AA676797 | *Cyclin F* |
| 16 | AA284072 | *CDK inhibitor 3 (CDK2-associated dual-specificity phosphatase)* |
| 17 | T81340 | *Defensin, α1, myeloid-related sequence* |
| 18 | AA430625 | *Dihydropyrimidine dehydrogenase* |
| 19 | R95732 | *DNA (cytosine-5)-methyltransferase 2* |
| 20 | R63623 | *Dual-specificity tyrosine phosphorylation−regulated kinase 2* |
| 21 | H63361 | *Expressed sequence tags* |
| 22 | H72875 | *GATA-binding protein 3* |
| 23 | AA478479 | *Heat shock protein (hsp110 family)* |
| 24 | AA625551 | *Homeobox A7* |
| 25 | AA504492 | *H. sapiens cDNA FLJ11997 fis, clone HEMBB1001458* |
| 26 | W20487 | *H. sapiens mRNA full-length insert cDNA clone EUROIMAGE 327506* |
| 27 | H44953 | *H. sapiens mRNA; cDNA DKFZp586A181 (from clone DKFZp586A181); partial cds* |
| 28 | AA011189 | *Homologue of yeast DNA cross-link repair gene SNM1; KIAA0086 gene product* |
| 29 | R10285 | *Hyaluronan-mediated motility receptor (RHAMM)* |
| 30 | H82442 | *Inhibitor of DNA binding 2, dominant-negative helix-loop-helix protein* |
| 31 | AA043806 | *Integrin $\beta_3$−binding protein ($\beta_3$-endonexin)* |
| 32 | AA029934 | *Integrin, $\alpha_V$ (vitronectin receptor, α polypeptide, antigen CD51)* |
| 33 | AA411324 | *Interleukin-13 receptor, α1* |
| 34 | AA150532 | *Keratin 6A* |
| 35 | AA420990 | *KIAA0033 protein* |
| 36 | AA677706 | *Lactotransferrin* |
| 37 | H28922 | *MCF2 cell line−derived transforming sequence-like* |
| 38 | N66177 | *Microphthalmia-associated transcription factor* |
| 39 | AA219061 | *mutS (Escherichia coli) homologue 2 (colon cancer, nonpolyposis type 1)* |
| 40 | AA703058 | *Myeloperoxidase* |
| 41 | AA286908 | *Myxovirus (influenza) resistance 2, homologue of murine* |
| 42 | W93379 | *NIMA (never in mitosis gene a)−related kinase 2* |
| 43 | AI002664 | *Phosphatidylinositol 4-kinase, catalytic, α polypeptide* |
| 44 | AA629262 | *Polo (Drosophila)−like kinase* |
| 45 | R40057 | *Prominin (mouse)−like 1* |
| 46 | AA453998 | *Protein phosphatase 3 (formerly 2B), catalytic subunit, α isoform (calcineurin A α)* |
| 47 | R46609 | *Protein tyrosine phosphatase, nonreceptor type 13 [APO-1/CD95 (Fas)−associated phosphatase]* |
| 48 | N55067 | *RAD23 (S. cerevisiae) homologue B* |
| 49 | AA486277 | *Retinoblastoma-binding protein 5* |
| 50 | N50554 | *Retinoblastoma-like 2 (p130)* |
| 51 | N47967 | *Rho GTPase-activating protein 5* |
| 52 | H81024 | *Serine/threonine kinase 12* |
| 53 | T95014 | *Serine/threonine kinase 4* |
| 54 | R73608 | *Solute carrier family 16 (monocarboxylic acid transporters) member 4* |
| 55 | AA454971 | *Ste20-related serine/threonine kinase* |
| 56 | R34694 | *TATA box binding protein−associated factor, RNA polymerase II, B, 150 kDa* |
| 57 | AA504348 | *Topoisomerase (DNA) IIα (170 kDa)* |
| 58 | AI337292 | *TTK protein kinase* |
| 59 | W92764 | *TNF-α-induced protein 6* |
| 60 | AA628154 | *Tumor protein p53-binding protein* |
| 61 | AA430504 | *Ubiquitin carrier protein E2-C* |
| 62 | H20676 | *Ubiquitin COOH-terminal hydrolase UCH37* |
| 63 | R39148 | *X-ray repair complementing defective repair in Chinese hamster cells 4* |
| 64 | AA406372 | *Zinc finger protein, X-linked* |

exposure appear in the sub-$G_1$ (apoptotic) compartment of the DNA distribution histograms. These data are consistent with our previous report demonstrating both rapid induction of apoptosis in HL60 cells in S phase during camptothecin treatment and recruitment of cells from the $G_1$ compartment using BrdUrd labeling (24).

## Discussion

We sought to elucidate whether CPT-11 alters expression of genes associated with cell cycle or apoptosis as a basis for its synergy with other chemotherapy drugs. Gene expression profiles were analyzed in human leukemia cells following *in vitro* exposure to SN-38, the active metabolite of CPT-11, and following *in vivo* therapy with CPT-11. Gene transcription profiles observed *in vitro* were compatible

with temporary delay of $G_1$-S cell cycle transition, loss of S-phase cells, unperturbed $G_2$-M-$G_1$ cycle transition, and enhanced apoptotic response, and similar drug-induced changes were detected for selected genes following treatment *in vivo*. To our knowledge, this is the first demonstration that specific pharmacogenomic effects detected by gene expression profiling *in vitro* following exposure to SN-38 also occur *in vivo* following administration of CPT-11.

Cell cycle–related changes included down-regulation of cyclin A2 and CDC2 and subsequent restoration to control values at 12 hours. These changes are consistent with the loss of S-phase cells, temporary $G_1$-S block, and subsequent reentry into S phase shown in the DNA distribution studies following exposure to SN-38. Cyclin A2 regulates the $G_1$-S- and $G_2$-M-phase transitions in the eukaryotic cell cycle by binding to and activating CDC2 (25, 26). The temporary down-regulation of genes

**Table 5. Genes up-regulated in all seven data sets: two sets of HL60 exposed to 0.1 and 0.3 μmol/L SN-38, one set of HL60 cells following exposure to 1.0 μmol/L SN-38, one set of an AML patient following *in vivo* treatment with 10 mg/m$^2$ CPT-11, and one set of a CML patient following *in vivo* treatment with 15 mg/m$^2$ CPT-11**

| | Name | Threshold level $\log_2$ (transcription drug-treated cells/transcription control cells) | | | | | |
|---|---|---|---|---|---|---|---|
| | | ≥0.5 | ≥0.6 | ≥0.7 | ≥0.8 | ≥0.9 | ≥1.0 |
| 1 | *Aminomethyltransferase (glycine cleavage system protein T)* | x | x | | | | |
| 2 | *BTG family member 2* | x | x | x | | | |
| 3 | *Cadherin 1, type 1, E-cadherin (epithelial)* | x | | | | | |
| 4 | *CD4 antigen (p55)* | x | | | | | |
| 5 | *Coagulation factor III (thromboplastin, tissue factor)* | x | x | | | | |
| 6 | *Core promoter element binding protein* | x | | | | | |
| 7 | *CDK(CDC2-like) 10* | x | | | | | |
| 8 | *Cytochrome P450, subfamily IID (debrisoquine, sparteine, etc., metabolizing), polypeptide 7a (pseudogene)* | x | | | | | |
| 9 | *Cytokine-inducible kinase* | x | x | x | | | |
| 10 | *Fas-activated serine/threonine kinase* | x | | | | | |
| 11 | *FOS-like antigen 2* | x | | | | | |
| 12 | *Growth arrest–specific 6* | x | x | | | | |
| 13 | *H2A histone family member X* | x | x | x | | | |
| 14 | *High-mobility group (nonhistone chromosomal) protein isoforms I and Y* | x | | | | | |
| 15 | *Histone deacetylase 3* | x | x | x | | | |
| 16 | *IFN-stimulated transcription factor 3, γ(48 kDa)* | x | | | | | |
| 17 | *junB proto-oncogene* | x | | | | | |
| 18 | *Low-density lipoprotein receptor (familial hypercholesterolemia)* | x | | | | | |
| 19 | *MHC class I polypeptide-related sequence A* | x | | | | | |
| 20 | *Phosphatase and tensin homologue (mutated in multiple advanced cancers 1)* | x | x | | | | |
| 21 | *Plasminogen activator, tissue* | x | | | | | |
| 22 | *Putative chemokine receptor; GTP-binding protein* | x | | | | | |
| 23 | *Serum/glucocorticoid–regulated kinase* | x | x | | | | |
| 24 | *Small inducible cytokine subfamily A (Cys-Cys) member 20* | x | | | | | |
| 25 | *Transferrin receptor (p90, CD71)* | x | | | | | |
| 26 | *TNFSF9* | x | x | x | x | x | x |
| 27 | *TNFSF2* | x | x | | | | |
| 28 | *TNFRSF10B* | x | | | | | |
| 29 | *TNFRSF7* | x | | | | | |
| 30 | *v-fos FBJ murine osteosarcoma viral oncogene homologue* | x | x | x | x | | |
| 31 | *Zinc finger protein 42 (myeloid-specific retinoic acid responsive)* | x | x | | | | |
| *n* | | 31 | 13 | 6 | 2 | 1 | 1 |

NOTE: Six different threshold levels were used to assess how stringency would affect the number of genes up-regulated in all seven data sets.

**Table 6. Genes down-regulated in all seven data sets (two sets of HL60 exposed to 0.1 and 0.3 μmol/L SN-38, one set of HL60 cells following exposure to 1.0 μmol/L SN-38, one set of an AML patient following *in vivo* treatment with 10 mg/m$^2$ CPT-11, and one set of a CML patient following *in vivo* treatment with 15 mg/m$^2$ CPT-11)**

| | Name | Threshold level $\log_2$ (transcription drug-treated cells/transcription control cells) | | | | | |
|---|---|---|---|---|---|---|---|
| | | ≤ −0.5 | ≤ −0.6 | ≤ −0.7 | ≤ −0.8 | ≤ −0.9 | ≤ −1.0 |
| 1 | *Adenomatosis polyposis coli* | x | x | x | x | x | x |
| 2 | *BIRC5 (survivin)* | x | x | x | x | x | x |
| 3 | *Budding uninhibited by benzimidazoles 1 (yeast homologue)* | x | | | | | |
| 4 | *Cyclic AMP–responsive element modulator* | x | | | | | |
| 5 | *CDC2, $G_1$-S and $G_2$-M* | x | | | | | |
| 6 | *Centromere protein E (312 kDa)* | x | x | x | x | x | x |
| 7 | *Centromere protein F (350/400 kDa, mitosin)* | x | x | x | x | | |
| 8 | *Cyclin A2* | x | x | x | x | x | x |
| 9 | *Cyclin B2* | x | x | x | x | x | x |
| 10 | *DEK oncogene (DNA binding)* | x | | | | | |
| 11 | *Deleted in lymphocytic leukemia, 2* | x | x | | | | |
| 12 | *H2A histone family member L* | x | x | x | x | | |
| 13 | *High-mobility group (nonhistone chromosomal) protein 17* | x | | | | | |
| 14 | *Human SH3 domain–containing protein SH3P18 mRNA, complete cds* | x | x | | | | |
| 15 | *Hyaluronan-mediated motility receptor (RHAMM)* | x | x | x | | | |
| 16 | *Inhibitor of DNA binding 2, dominant-negative helix-loop-helix protein* | x | | | | | |
| 17 | *MAD2 (mitotic arrest deficient, yeast, homologue)–like 1* | x | x | x | | | |
| 18 | *Minichromosome maintenance deficient (S. cerevisiae) 4* | x | | | | | |
| 19 | *NIMA (never in mitosis gene a)–related kinase 2* | x | | | | | |
| 20 | *Nuclear receptor corepressor/histone deacetylase3 complex subunit* | x | x | | | | |
| 21 | *Phosphodiesterase 4B, cyclic AMP–specific [dunce (Drosophila) homologuephosphodiesterase E4]* | x | | | | | |
| 22 | *Protein phosphatase 3 (formerly 2B), catalytic subunit,α isoform (calcineurin Aα)* | x | | | | | |
| 23 | *Topoisomerase (DNA) IIα (170 kDa)* | x | x | x | x | x | x |
| 24 | *TRAF family member–associated nuclear factor-κB activator* | x | | | | | |
| 25 | *TTK protein kinase* | x | | | | | |
| 26 | *Ubiquitin carrier protein E2-C* | x | x | x | x | x | x |
| 27 | *v-yes-1 Yamaguchi sarcoma viral oncogene homologue1* | x | | | | | |
| 28 | *X-ray repair complementing defective repair in Chinese hamster cells 4* | x | | | | | |
| *n* | | 28 | 14 | 11 | 9 | 7 | 7 |

NOTE: Six different threshold levels were used to assess how stringency would affect the number of genes down-regulated in all seven data sets.

with constant expression throughout the cell cycle, such as *CDC7-like 1* (*CDC7*) and *v-abl Abelson murine leukemia viral oncogene homologue 1*, is also consistent with SN-38-induced loss of S-phase cells. Cyclin F is thought to be involved in the $G_2$ cell cycle phase based on the accumulation of cyclin F protein during interphase and its subsequent rapid degradation (27). The observed down-regulation of *cyclin F* following exposure of HL60 cells to SN-38 and its slow recovery to control levels are consistent with a temporary lack of

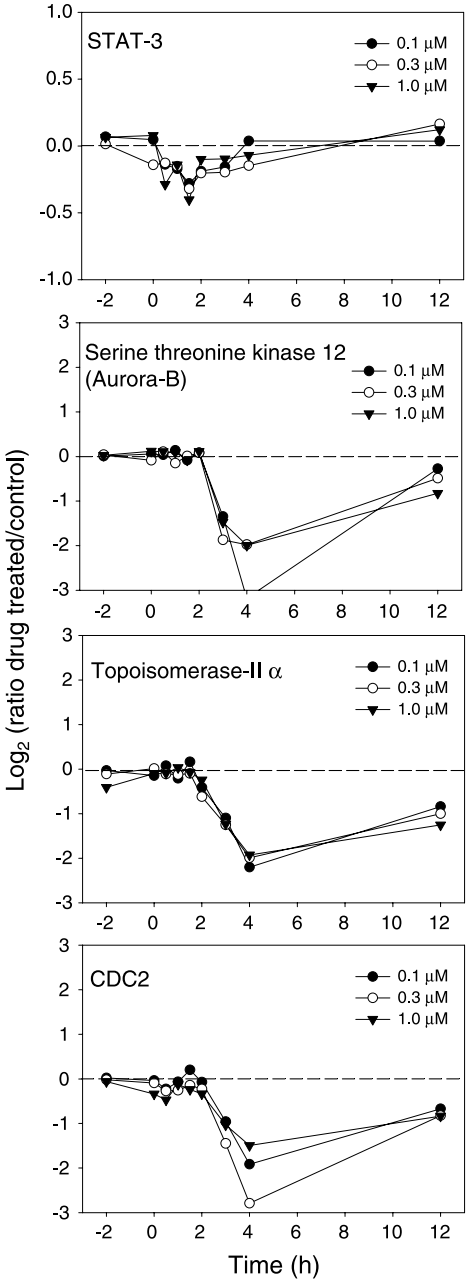


**Figure 4.** Time kinetic analysis of transcription of genes in the survivin pathway in HL60 cells before, during, and following 2-h *in vitro* exposure to 0.1, 0.3, and 1.0 μmol/L SN-38. The drug exposure was initiated at −2 h and was stopped at 0 h. Expression in drug-treated cells was compared with that in control cells sampled at the same time points. Note that the *Y axis* scale for signal transducers and activators of transcription 3 (*STAT-3*) ranges from −1 to 1, whereas the other graphs range from −3 to 3.

recruitment of cells into $G_2$. This is further supported by the temporary reduction of expression of genes encoding $G_2$-M-phase–specific proteins, such as *CDC27* (28), *centromere protein E* (29), and *kinesin-like 5* (*CHO1*; ref. 30). CDC27 is a component of the so-called anaphase-promoting complex that plays an essential role in the metaphase-to-anaphase transition. Centromere protein E and kinesin-like 5 are kinesin-like motor proteins that are involved in transport of organelles within cells and movement of chromosomes during cell division.

Other changes consistent with a temporary SN-38-induced block in $G_1$-S transition include temporary down-regulation of *CDK4* and increased expression of *BTG family member 2* and *BCL6*. CDK4 is a catalytic subunit of the protein kinase complex that is important for cell cycle $G_1$-phase progression (31). The activity of this kinase is restricted to the $G_1$-S phase. CDK4 is required for cell cycle progression; it phosphorylates the retinoblastoma gene product (Rb) and inactivates its repressor function. Following SN-38 exposure, *CDK4* expression in HL60 decreases slightly, reaching its nadir 1 hour following drug exposure and subsequently returning to normal levels at 12 hours. The expression kinetics of *CDK inhibitor 2A (p16)*, which inhibits CDK-4 (32), are opposite to those observed for *CDK-4*, suggesting

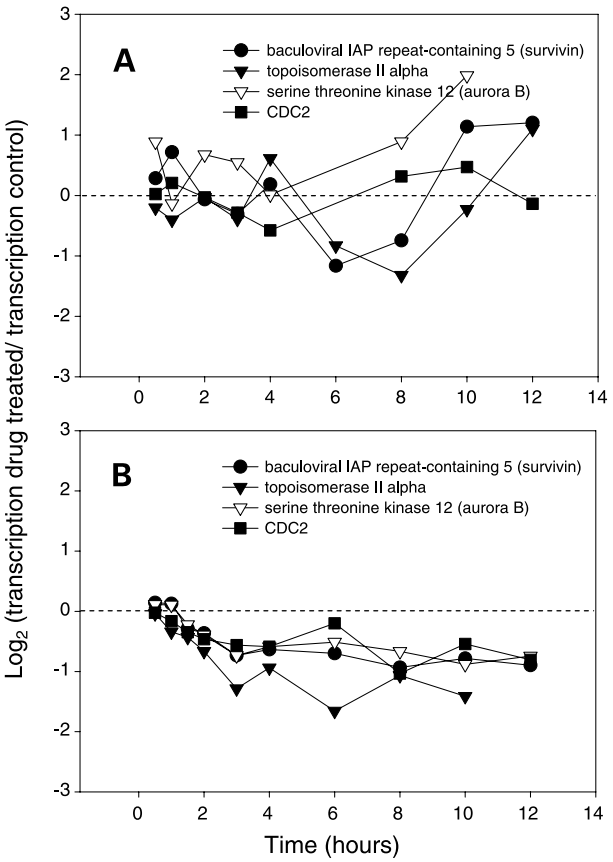


**Figure 5.** Time kinetic analysis of transcription of genes in the survivin pathway following *in vivo* treatment of an AML patient with 10 mg/m$^2$ CPT-11 (**A**) and a CML in myeloid blast transformation patient with 15 mg/m$^2$ CPT-11 (**B**). Gene expression at each time point was compared with expression in a sample obtained immediately before the start of the CPT-11 infusion (0 h).

**Table 7. Validation of mRNA expression levels in HL60 cells 6 hours after a 2-hour exposure to SN-38 determined by real-time quantitative reverse transcription-PCR**

| SN-38 concentration (μmol/L) | Survivin/β-actin, mean ± SD ($\times 10^{-3}$) | Fold change compared with control | TNFSF9/β-actin, mean ± SD ($\times 10^{-3}$) | Fold change compared with control |
|---|---|---|---|---|
| 0 | 269.58 ± 17.70 | 1 | 12.09 ± 1.48 | 1 |
| 0.1 | 187.44 ± 9.15 | 0.7 | 20.13 ± 3.33 | 1.7 |
| 0.3 | 151.53 ± 6.84 | 0.56 | 26.25 ± 3.96 | 2.2 |
| 1.0 | 135.80 ± 15.70 | 0.50 | 43.31 ± 3.16 | 3.6 |

NOTE: Each value is presented as the mean ± SD of triplicate experiments.

a causal relationship. SN-38 exposure also leads to rapid up-regulation of *BTG family member 2* and *BCL6,* with subsequent slow decrease to control levels. BTG family member 2 belongs to a family of structurally related proteins that seem to have antiproliferative properties and are involved in the regulation of the $G_1$-S transition of the cell cycle (33). BCL6 is a zinc finger transcription factor that acts as a sequence-specific repressor of transcription (34).

Proapoptotic changes in gene expression following SN-38 exposure included down-regulation of *BCL2*, an integral inner mitochondrial membrane protein that blocks apoptotic death (35), and up-regulation of *BCL10,* which encodes a protein with a caspase recruitment domain and has been shown to induce apoptosis (36). Increased expression was also observed for *BCL2/adenovirus E1B 19-kDa interacting protein 3*, *TNFRSF10B (death receptor 5)*, *TNFSF2*, *TNFSF9 (4-1 BB-L)*, *caspase-6 apoptosis-related cysteine protease,* and *TRAF family member–associated nuclear factor-κB activator/TRAF.* BCL2/adenovirus E1B 19-kDa interacting protein 3 is a member of the BCL2/adenovirus E1B 19-kDa interacting protein family and has been associated with proapoptotic function (37). The dimeric mitochondrial protein encoded by this gene is known to induce apoptosis even in the presence of BCL2. It binds antiapoptotic viral E1B 19-kDa protein and cellular Bcl2 protein. The protein encoded by *TNFRSF10B* is a member of the TNFRSF and is involved in apoptosis signal transduction (38). The *TNF* gene encodes a multifunctional proinflammatory cytokine that belongs to the TNFSF and is involved in the regulation of a wide spectrum of biological processes, including cell proliferation and apoptosis (38). The protein encoded by *TNFSF9* is a TNF-related ligand that induces activated T lymphocytes to proliferate and is involved in antigen presentation (39). *Caspase-6 apoptosis-related cysteine protease* encodes a protein that is a member of the cysteine-aspartic acid protease (caspase) family. Sequential activation of

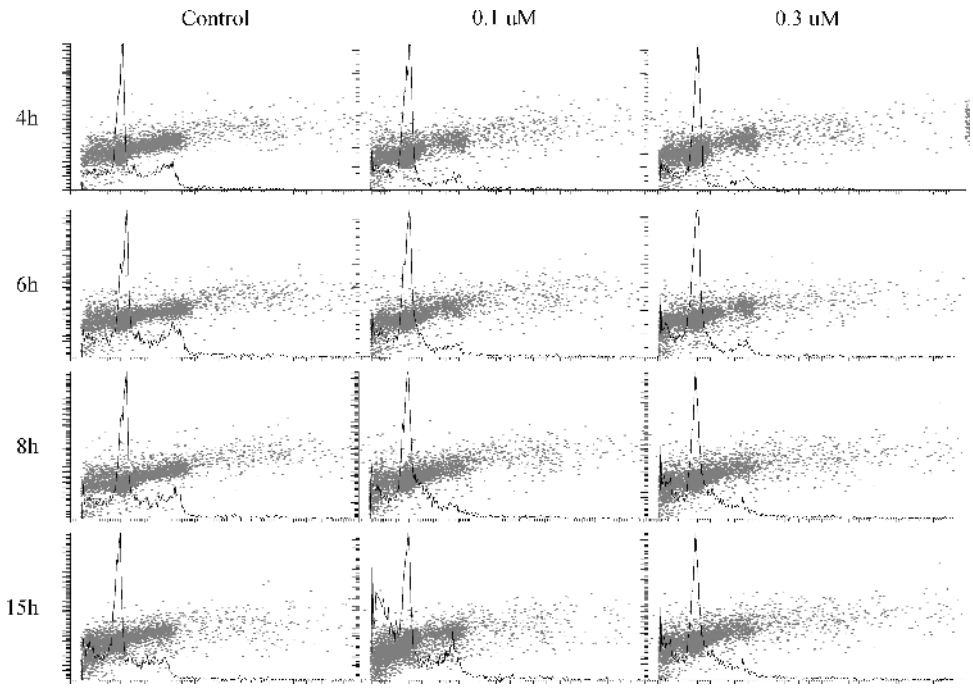


**Figure 6.** DNA distribution of HL60 cells following 2-h exposure to 0.1 and 0.3 μmol/L SN-38. The different drug concentrations are shown in columns, and the different sampling time points are shown in rows. Single-variable histograms of DNA content are superimposed on two-variable dot plots of side scatter (*Y axis*) versus DNA content (*X axis*).

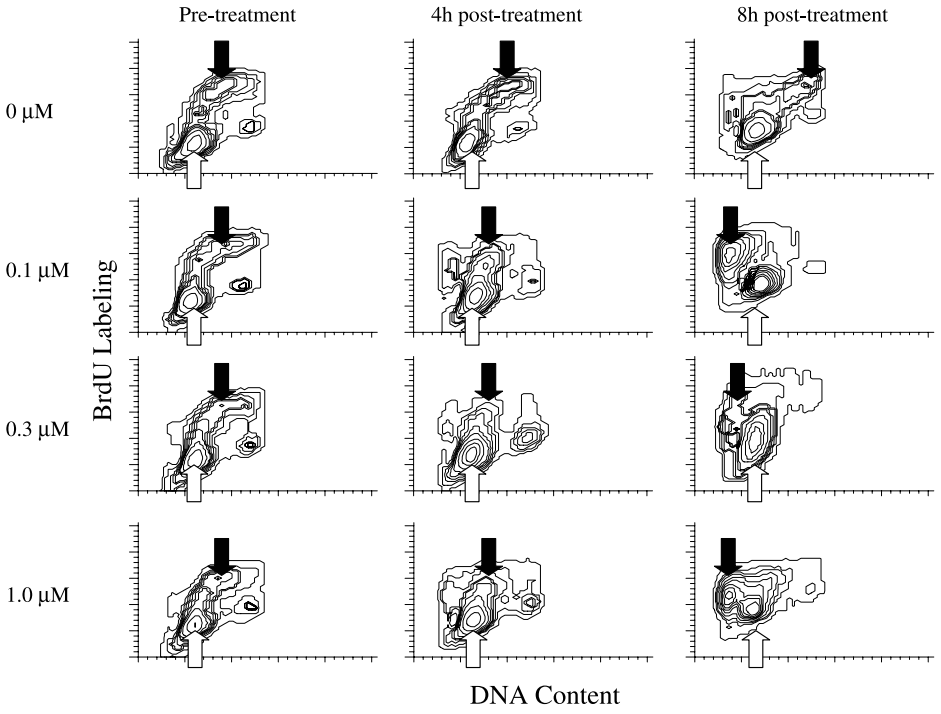


**Figure 7.** Time kinetic analysis of BrdUrd-labeled S-phase cells following exposure to SN-38. Each *row* shows bivariate plots of BrdUrd labeling versus DNA content of control cells and cells exposed to 0.1, 0.3, and 1.0 μmol/L SN-38, respectively, sampled at 0 h (*left*), 4 h (*middle*), and 8 hours (*right*) following a 2-h drug exposure. In the control cultures, BrdUrd-labeled cells traverse the cell cycle from S phase toward the $G_2$-M and subsequent $G_1$ phase, whereas the fate of the S-phase BrdUrd-labeled cells in the SN-38-treated cell population exposure is the sub-$G_1$ (apoptotic) compartment of the DNA distribution histograms. The position of the $G_1$ population in each plot is marked with a white arrow, whereas the position of the BrdUrd-labeled cells (cells that were in S phase before drug treatment) is marked by a black arrow.

caspases plays a central role in the execution phase of cell apoptosis, and caspase-6 apoptosis-related cysteine protease is thought to function as a downstream enzyme in the caspase activation cascade (40). The TRAF family of proteins associate with and transduce signals from members of the TNFRSF and are required for TNF receptor signaling (41). These proapoptotic molecular responses observed in our study are in line with published CPT-11/SN-38 augmentation of extrinsic apoptotic response signal transduction pathways (12–17).

Down-regulation of *BIRC5 (survivin)* was also observed following CPT-11/SN-38 exposure *in vitro* and *in vivo*. The protein encoded by this gene is an apoptosis inhibitor that is expressed during the $G_2$-M phase of the cell cycle. BIRC5 associates with the microtubules of the mitotic spindle, and any disruption results in the loss of apoptosis activity (42). Inhibition of signal transducers and activators of transcription 3 (STAT3) signaling has been described to induce apoptosis and decrease survivin expression in primary effusion lymphoma (43). Downstream, survivin stimulates Aurora-B kinase (serine/threonine kinase) activity and helps correctly target Aurora-B to its substrates during the cell cycle (44). One of the substrates targeted by Aurora-B is topoisomerase IIα (45). Recently, it has been suggested that an approach to targeting survivin in cancer therapy is the use of CDC2 antagonists, because CDC2 phosphorylates survivin at the $Thr^{34}$ position (42). The microarray analysis showed that SN-38 down-regulates STAT3, *Aurora-B kinase, topoisomerase IIα,* and *CDC2,* suggesting that CPT-11 may be an interesting candidate for pharmacologic targeting of survivin.

In addition to proapoptotic changes in gene expression, antiapoptotic changes were also observed. Of note, SN-38 exposure induced up-regulation of *BCL2-related protein A1 (BCL2A)* and *BCL2-like 2 (bcl-w)*. The protein encoded by BCL2-related protein A1 reduces cytochrome *c* release from mitochondria and blocks caspase activation (46). Expression of BCL2-like 2 in cells has been shown to reduce apoptosis (47). Biological responses are commonly controlled by a balance between stimulatory and inhibitory mechanisms, and the preponderance of proapoptotic signals following SN-38 exposure suggests that the antiapoptotic changes may be relatively inconsequential.

It should be noted that although some of the fold changes in expression detected were small (e.g., in the survivin-associated genes *in vivo*) the patterns shown by the kinetic analysis gave support to the concept that the observed increases and decreases in expression were true time-dependent changes rather than background noise, while this conclusion could not have been drawn from studying only a single posttreatment sample. However, it will be necessary to determine what levels of changes are associated with biologically significant responses.

The gene expression data reported here have implications for the use of CPT-11 in combination regimens. Demonstration of changes in expression of cell cycle–related genes induced by SN-38, associated with a temporary delay of $G_1$-S transition, corroborates a sequence-dependent synergistic interaction of this drug with S-phase–specific agents. In addition, demonstration of proapoptotic changes in gene expression corroborates the sequence-dependent synergistic interaction of SN-38

with inducers of extrinsic apoptotic pathways, such as TNF-related apoptosis-inducing ligand/Apo2L. In addition, the *in vitro* and *in vivo* effects of SN-38/CPT-11 on the survivin pathway suggest that the proapoptotic effects of SN-38 may not be restricted to the extrinsic apoptotic pathway. Further studies may be helpful in optimizing the timing of combination regimens.

This is, to our knowledge, the first study comparing changes in gene transcription profiles induced by SN-38 *in vitro* and CPT-11 *in vivo*. Future studies will seek to increase the sophistication of analysis of changes in gene expression. Moreover, to fully comprehend the significance of the observed gene transcription changes, correlative studies of protein expression and phosphorylation are required and additional correlative studies are required to associate changes in gene and protein expression with biological responses. The continual enhancement of bioinformatic analysis programs and the further development of high-throughput techniques in these areas are expected to facilitate these comprehensive studies in the very near future.

### References


**1.** Masuda N, Fukuoka M, Kusunoki Y, et al. CPT-11: a new derivative of camptothecin for the treatment of refractory or relapsed small-cell lung cancer. J Clin Oncol 1992;10:1225 – 9.

**2.** Ohno R, Okada K, Masaoka T, et al. An early phase II study of CPT-11: a new derivative of camptothecin, for the treatment of leukemia and lymphoma. J Clin Oncol 1990;8:1907 – 12.

**3.** Rougier P, Bugat R, Douillard JY, et al. Phase II study of irinotecan in the treatment of advanced colorectal cancer in chemotherapy-naive patients and patients pretreated with fluorouracil-based chemotherapy. J Clin Oncol 1997;15:251 – 60.

**4.** Conti JA, Kemeny NE, Saltz LB, et al. Irinotecan is an active agent in untreated patients with metastatic colorectal cancer. J Clin Oncol 1996; 14:709 – 15.

**5.** Pitot HC, Wender DB, O'Connell MJ, et al. Phase II trial of irinotecan in patients with metastatic colorectal carcinoma. J Clin Oncol 1997;15: 2910 – 9.

**6.** Shimada Y, Yoshino M, Wakui A, et al. Phase II study of CPT-11, a new camptothecin derivative, in metastatic colorectal cancer. CPT-11 Gastrointestinal Cancer Study Group. J Clin Oncol 1993;11:909 – 13.

**7.** Rothenberg ML, Eckardt JR, Kuhn JG, et al. Phase II trial of irinotecan in patients with progressive or rapidly recurrent colorectal cancer. J Clin Oncol 1996;14:1128 – 35.

**8.** Guichard S, Hennebelle I, Bugat R, Canal P. Cellular interactions of 5-fluorouracil and the camptothecin analogue CPT-11 (irinotecan) in a human colorectal carcinoma cell line. Biochem Pharmacol 1998;55: 667 – 76.

**9.** Pavillard V, Formento P, Rostagno O, et al. Combination of irinotecan (CPT-11) and 5-fluorouracil with an analysis of cellular determinants of drug activity. Biochem Pharmacol 1998;56:1315 – 22.

**10.** Xu JM, Azzariti A, Tommasi S, et al. Combination of 5-fluorouracil and irinotecan on modulation of thymidylate synthase and topoisomerase I expression and cell cycle regulation in human colon cancer LoVo cells: clinical relevance. Clin Colorect Cancer 2002; 2:182 – 8.

**11.** Naka T, Sugamura K, Hylander BL, Widmer MB, Rustum YM, Repasky EA. Effects of tumor necrosis factor-related apoptosis-inducing ligand alone and in combination with chemotherapeutic agents on patients' colon tumors grown in SCID mice. Cancer Res 2002;62: 5800 – 6.

**12.** Gliniak B, Le T. Tumor necrosis factor-related apoptosis-inducing ligand's antitumor activity *in vivo* is enhanced by the chemotherapeutic agent CPT-11. Cancer Res 1999;59:6153 – 8.

**13.** Xiang H, Fox JA, Totpal K, et al. Enhanced tumor killing by Apo2L/TRAIL and CPT-11 co-treatment is associated with p21 cleavage and differential regulation of Apo2L/TRAIL ligand and its receptors. Oncogene 2002;21:3611 – 9.

**14.** Cao S, Rustum Y. Synergistic antitumor activity of irinotecan in combination with 5-fluorouracil in rats bearing advanced colorectal cancer: role of drug sequence and dose. Cancer Res 2000;60:3717 – 21.

**15.** Lin T, Zhang L, Davis J, et al. Combination of TRAIL genetherapy and chemotherapy enhances antitumor and antimetastasis effects in chemosensitive and chemoresistant breast cancers. Mol Ther 2003;8: 441 – 8.

**16.** Ray S, Almasan A. Apoptosis induction in prostate cancer cells and xenografts by combined treatment with Apo2 ligand/tumor necrosis factor-related apoptosis-inducing ligand and CPT-11. Cancer Res 2003; 63:4713 – 23.

**17.** Keane MM, Ettenberg SA, Nau MM, Russell EK, Lipkowitz S. Chemotherapy augments TRAIL-induced apoptosis in breast cell lines. Cancer Res 1999;59:734 – 41.

**18.** Goldwasser F, Bae I, Valenti M, Torres K, Pommier Y. Topoisomerase I-related parameters and camptothecin activity in the colon carcinoma cell lines from the National Cancer Institute anticancer screen. Cancer Res 1995;55:2116 – 21.

**19.** Zhou Y, Gwadry FG, Reinhold WC, et al. Transcriptional regulation of mitotic genes by camptothecin-induced DNA damage: microarray analysis of dose- and time-dependent effects. Cancer Res 2002;62: 1688 – 95.

**20.** Zhumabayeva B, Diatchenko L, Chenchik A, Siebert PD. Use of SMART-generated cDNA for gene expression studies in multiple human tumors. Biotechniques 2001;30:158 – 63.

**21.** Zhu G, Reynolds L, Crnogorac-Jurcevic T, et al. Combination of microdissection and microarray analysis to identify gene expression changes between differentially located tumour cells in breast cancer. Oncogene 2003;22:3742 – 8.

**22.** Hector S, Bolanowska-Higdon W, Zdanowicz J, Hitt S, Pendyala L. *In vitro* studies on the mechanisms of oxaliplatin resistance. Cancer Chemother Pharmacol 2001;48:398 – 406.

**23.** Bunworasate U, Arnouk H, Minderman H, et al. Erythropoietin-dependent transformation of myeloplastic syndrome to acute monoblastic leukemia. Blood 2001;98:3492 – 4.

**24.** Minderman H, Cao S, Rustum YM. Rational design of CPT-11 (irinotecan) administration based on preclinical *in vitro* and *in vivo* models. Oncology 1998;12:22 – 30.

**25.** Blanchard JM. Cyclin A2 transcriptional regulation: modulation of cell cycle control at the $G_1$-S transition by peripheral cues. Biochem Pharmacol 2000;60:1179 – 84.

**26.** Porter LA, Donoghue DJ. Cyclin B1 and CDK1: nuclear localization and upstream regulators. Prog Cell Cycle Res 2003;5:335 – 47.

**27.** Fung TK, Siu WY, Yam CH, Lau A, Poon RY. Cyclin F is degraded during $G_2$-M by mechanisms fundamentally different from other cyclins. J Biol Chem 2002;277:35140 – 9.

**28.** Topper LM, Campbell MS, Tugendreich S, et al. The dephosphorylated form of the anaphase-promoting complex protein Cdc27/Apc3 concentrates on kinetochores and chromosome arms in mitosis. Cell Cycle 2002;1:282 – 92.

**29.** Schaar BT, Chan GK, Maddox P, Salmon ED, Yen TJ. CENP-E function at kinetochores is essential for chromosome alignment. J Cell Biol 1997; 139:1373 – 82.

**30.** Kuriyama R, Gustus C, Terada Y, Uetake Y, Matuliene J. CHO1, a mammalian kinesin-like protein, interacts with F-actin and is involved in the terminal phase of cytokinesis. J Cell Biol 2002;156:783 – 90.

**31.** Sherr CJ, Roberts JM. CDK inhibitors: positive and negative regulators of $G_1$-phase progression. Genes Dev 1999;13:1501 – 12.

**32.** Gump J, Stokoe D, McCormick F. Phosphorylation of p16INK4A correlates with Cdk4 association. J Biol Chem 2003;278:6619 – 22.

**33.** Duriez C, Falette N, Audoynaud C, et al. The human BTG2/TIS21/PC3 gene: genomic structure, transcriptional regulation and evaluation as a candidate tumor suppressor gene. Gene 2002;282:207 – 14.

**34.** Albagli-Curiel O. Ambivalent role of BCL6 in cell survival and transformation. Oncogene 2003;22:507 – 16.

**35.** Cory S, Adams JM. The Bcl2 family: regulators of the cellular life-or-death switch. Nat Rev Cancer 2002;2:647 – 56.

**36.** Maes B, Demunter A, Peeters B, De Wolf-Peeters C. BCL10

mutation does not represent an important pathogenic mechanism in gastric MALT-type lymphoma, and the presence of the API2-MLT fusion is associated with aberrant nuclear BCL10 expression. Blood 2002;99: 1398 – 404.

**37.** Ray R, Chen G, Vande Velde C, et al. BNIP3 heterodimerizes with Bcl-2/Bcl-X(L) and induces cell death independent of a Bcl-2 homology 3 (BH3) domain at both mitochondrial and nonmitochondrial sites. J Biol Chem 2000;275:1439 – 48.

**38.** Thorburn A. Death receptor-induced cell killing. Cell Signal 2004;16: 139 – 44.

**39.** Salih HR, Kiener PA, Nussler V. 4-1 BB ligand—just another costimulating molecule? Int J Clin Pharmacol Ther 2002;40:348 – 53.

**40.** Degterev A, Boyce M, Yuan J. A decade of caspases. Oncogene 2003;22:8543 – 67.

**41.** Aggarwal BB. Signalling pathways of the TNF superfamily: a double-edged sword. Nat Rev Immunol 2003;3:745 – 56.

**42.** Altieri DC. Validating survivin as a cancer therapeutic target. Nat Rev Cancer 2003;3:46 – 54.

**43.** Aoki Y, Feldman GM, Tosato G. Inhibition of STAT3 signaling induces apoptosis and decreases survivin expression in primary effusion lymphoma. Blood 2003;101:1535 – 42.

**44.** Chen J, Jin S, Tahir SK, et al. Survivin enhances Aurora-B kinase activity and localizes Aurora-B in human cells. J Biol Chem 2003;278: 486 – 90.

**45.** Morrison C, Henzing AJ, Jensen ON, et al. Proteomic analysis of human metaphase chromosomes reveals topoisomerase IIα as an Aurora B substrate. Nucleic Acids Res 2002;30:5318 – 27.

**46.** Werner AB, de Vries E, Tait SW, Bontjer I, Borst J. Bcl-2 family member Bfl-1/A1 sequesters truncated bid to inhibit is collaboration with pro-apoptotic Bak or Bax. J Biol Chem 2002;277:22781 – 8.

**47.** Gibson L, Holmgreen SP, Huang DC, et al. bcl-w, a novel member of the bcl-2 family, promotes cell survival. Oncogene 1996;13:665 – 75.

Molecular Cancer Therapeutics

# *In vitro* and *in vivo* irinotecan-induced changes in expression profiles of cell cycle and apoptosis-associated genes in acute myeloid leukemia cells

Hans Minderman, Jeffrey M. Conroy, Kieran L. O'Loughlin, et al.

*Mol Cancer Ther* 2005;4:885-900.